Cell Source-Specific Extracellular Vesicles Direct Zone-Specific MSC Differentiation for Rotator Cuff Enthesis Regeneration

Zizhao Li[1], Catherine Cheung[1], Lin Xu[1], Sung-Han Jo[1], Se-Hwan Lee[1], Jayden Shin[1], Felicia Pinto[1], Ellie MacMullan[1], Jina Ko[1], and Su Chin Heo[1]
[1]University of Pennsylvania, Philadelphia, PA
lizizhao@seas.upenn.edu

DISCLOSURES: Li (N), Cheung (N), Xu (N), Jo (N), Lee (N), Shin (N), Pinto (N), MacMullan (N), Ko (N), and Heo (5-4WEB Medical Inc.)

INTRODUCTION: The rotator cuff is essential for shoulder stability and mobility, yet tears at the tendon-to-bone insertion (enthesis) are highly prevalent and remain notoriously difficult to repair **[1]**. Despite advances in surgical techniques, re-tear rates remain high due to the formation of mechanically weak scar tissue, poor vascularization, and the inability to replicate the highly specialized, multi-zonal architecture of the native enthesis **[3–4]**. This tissue interface is composed of tendon, fibrocartilage, and bone regions, each defined by distinct biochemical and mechanical cues, underscoring the need for strategies that can address this structural complexity. Cell-based approaches have been explored to improve healing, but challenges with cell survival, delivery, and regulatory translation limit their clinical utility. Recently, extracellular vesicles (EVs), lipid-bound nanoparticles (50–200 nm) that carry functional RNAs, proteins and signaling molecules, have emerged as a promising alternative **[5]**. EVs offer many of the paracrine benefits of their parent cells while avoiding many of the logistical and safety barriers of direct cell therapies [**6**]. Notably, EVs from diverse cell sources have been shown to promote tenogenic and chondrogenic differentiation, making them particularly attractive for musculoskeletal repair **[7–10]**. In this work, we systematically characterized EVs derived from three enthesis-relevant cell types: tenocytes (T-EV), chondrocytes (C-EV), and mesenchymal stem cells (M-EV). We further examined their effects on MSC proliferation and lineage commitment to assess their therapeutic potential for promoting zone-specific regeneration of the rotator cuff enthesis.

METHODS: EVs were isolated from passage-1 juvenile bovine tenocytes (T-EV), chondrocytes (C-EV) and mesenchymal stem cells (M-EV) using our optimized ultracentrifugation protocol **(Fig. 1A) [11–12]**. Particle size and concentration were quantified by nanoparticle tracking analysis (NTA), and morphology was examined via scanning electron microscopy (SEM, FEI Quanta). EV identity was confirmed by immunostaining with tetraspanin markers (CD9, CD63, CD81) and validated by direct super-resolution stochastic optical reconstruction microscopy (dSTORM, ONI Nanoimager). EV uptake by recipient bovine MSCs (bMSCs) was assessed using DiO-labeled (DiO: a lipophilic carbocyanine DiOC18) EVs. For cell migration analysis, scratch closure assays were performed on passage-1 bMSCs treated with T-EV, C-EV, or M-EV (3×10^4 EV/cell), and wound closure was quantified over 24 h. Cell proliferation was assessed by seeding bMSCs with the same EV treatments and quantifying metabolic activity using the Cell Counting Kit-8 on Days 1 and 3. For differentiation analysis, bMSCs were treated with each EV type, followed by RNA extraction (TRIzol) and RT-qPCR to evaluate tendon, fibrocartilage, and cartilage-associated genes (COL1A2, COL2, COL3, Tenascin-C), normalized to GAPDH.

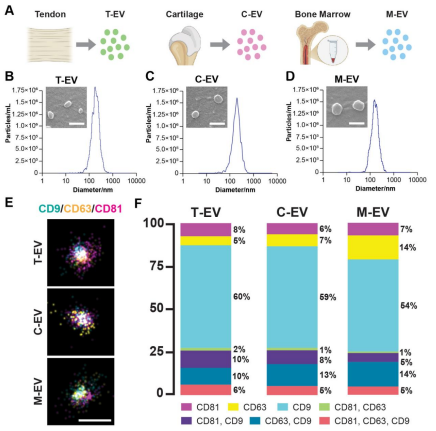

Fig. 1: (A) Schematic illustration of T-EV, C-EV and M-EV isolation process. (B-D) Quantitative NTA results and SEM images of T-EV, C-EV, and M-EV (scale bar = 200 nm). (E) Representative STORM images of individual T-EV, C-EV, and M-EV (Green: CD9, Yellow: CD63, Red: CD81; scale bar = 200 nm). (F) Tetraspanin co-localization analysis of T-EV, C-EV, and M-EV.

RESULTS: SEM confirmed successful isolation of T-EV, C-EV, and M-EV, which exhibited predominantly spherical to ovoid morphology with diameters <200 nm **(Fig. 1B-D)**. NTA analysis revealed mean particle sizes of 196.8 nm, 182.4 nm, and 195.2 nm, respectively. Super-resolution imaging (dSTORM) verified the presence of canonical EV tetraspanins (CD9, CD63, CD81) across all groups, with comparable distributions of single-, double-, and triple-positive subpopulations **(Fig. 1E-F)**. Among single-positive vesicles, CD9 predominated (T-EV: 60%, C-EV: 59%, M-EV: 54%), while CD9/CD63 was the most frequent double-positive subset (T-EV: 10%, C-EV: 13%, M-EV: 14%). DiO labeling demonstrated efficient uptake of all EV types by recipient bMSCs, with fluorescence distributed throughout the cytoplasm **(Fig. 2A)**. Functionally, EV supplementation significantly enhanced MSC motility, as evidenced by accelerated wound closure in scratch assays at 0 and 12 hours compared with untreated controls **(Fig. 2B-C).** Proliferation analysis revealed modest but consistent increases in MSC growth across all EV-treated groups, whereas control cells expanded more slowly over the same time points **(Fig. 2D)**. Gene expression analysis demonstrated distinct lineage-specific effects among the EV types. T-EV and M-EV treatment significantly upregulated Tenascin-C and COL3 compared to control and C-EV groups, reflecting enhanced tenogenic and fibrocartilaginous cues **(Fig. 3A)**. Notably, M-EV induced the highest expression of the chondrogenic marker COL2 (1.5–3-fold increase), whereas C-EV most strongly promoted COL1A2 expression **(Fig. 3A)**.

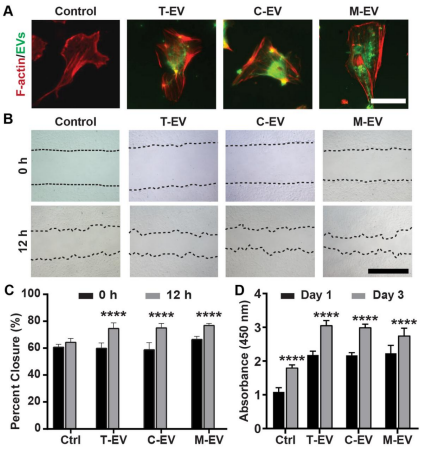

Fig. 2: (A) Representative fluorescence images of bMSCs treated with T-EV, C-EV, and M-EV (bar = 50 µm). (B) Representative images of scratch assay in bMSCs treated with T-EV, C-EV, and M-EV over 24 hours (scale bar = 1 mm). (C) Percent cell closure over 24 hours (*: $p < 0.05$, **: $p < 0.01$, ****: $p < 0.0001$). (D) Proliferation of bMSCs treated with T-EV, C-EV, and M-EV, determined by CCK8 assay (****: $p < 0.0001$, n = 5/group, mean ± SD).

DISCUSSION: This study systematically evaluated the functional potential of bovine-derived EVs from tenocytes (T-EV), chondrocytes (C-EV), and mesenchymal stem cells (M-EV) to direct MSC behavior in vitro, providing new insight into their application for rotator cuff enthesis repair. Comprehensively characterized confirmed nanoscale morphology and canonical tetraspanin markers across all EV types, which were efficiently internalized by MSCs without adverse effect. Functionally, all EV groups enhanced MSC migration and proliferation compared to untreated controls, underscoring their biocompatibility and general pro-regenerative effects. Importantly, gene expression profiling revealed source-dependent differentiation cues. M-EV strongly promoted chondrogenic and tenogenic markers, T-EVs favored tenogenic and fibrogenic signatures, and C-EV induced fibrous and cartilage-related genes. These results suggest that EV cargo reflects the molecular identity of the donor cell and can selectively bias MSC lineage commitment. Such source-dependent effects highlight the potential of EV-based therapies to achieve spatially tailored regeneration of the multi-zonal enthesis, where tendon, fibrocartilage, and bone must be restored in a coordinated manner. Future work will employ proteomic and transcriptomic profiling to define the molecular cargo of these vesicles and guide the design of zonal biomimetic scaffolds incorporating specific EV subtypes. Together, these findings establish EVs as promising non-cellular therapeutics capable of orchestrating zone-specific differentiation, addressing one of the major challenges in rotator cuff repair and tendon-to-bone integration.

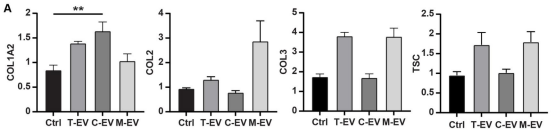

Fig. 3: Gene expression in bMSCs treated with T-EVs, C-EVs, and M-EVs on day 7, normalized to GAPDH (**: $p < 0.01$, n = 5/group, mean ± SD).

SIGNIFICANCE: This work establishes a non-cellular, EV-mediated strategy to promote lineage-specific differentiation of MSCs, offering a promising platform for zone-specific tendon-to-bone interface regeneration. By harnessing the intrinsic bioactivity of cell source–dependent EVs, and integrating them into biomaterial systems, this approach may overcome current limitations in enthesis repair and accelerate translation toward clinically relevant therapies.

REFERENCES: [1] Apostolakos+, *M.L.T.J.* 2014; [2] Sahoo+, *JSES Int.* 2015; [3] Sambandam+, *World J Orthop.* 2015; [4] Oh+, *Clin Orthop Surg.* 2018; [5] Nakase+, *Sci Rep.* 2016; [6] Zou+, *J. Nanobiotechnology* 2023; [7] Kodama+, *Bone Rep.* 2022; [8] Xu+, *CT.* 2019; [9] Yu+, *Acta Biomater.* 2020; [10] Connor+, *J. Bone Miner.* 2019; [11] Ko+, *Adv. Biosyst.* 2020; [12] Reynolds+, *J of Extracellular Bio.* 2023.

ACKNOWLEDGEMENTS: This work was supported by NIH (P50 AR080581) and NSF (CMMI-1548571).